

PDV: Prompt Directional Vectors for Zero-shot Composed Image Retrieval

Osman Tursun¹, Sinan Kalkan², Simon Denman¹ and Clinton Fookes¹

¹Queensland University of Technology

²Middle East Technical University

{osman.tursun, s.denman, c.fookes}@qut.edu.au, skalkan@metu.edu.tr

Abstract

*Zero-shot composed image retrieval (ZS-CIR) enables image search using a reference image and text prompt without requiring specialized text-image composition networks trained on large-scale paired data. However, current ZS-CIR approaches face three critical limitations in their reliance on composed text embeddings: static query embedding representations, insufficient utilization of image embeddings, and suboptimal performance when fusing text and image embeddings. To address these challenges, we introduce the **Prompt Directional Vector (PDV)**, a simple yet effective training-free enhancement that captures semantic modifications induced by user prompts. PDV enables three key improvements: (1) dynamic composed text embeddings where prompt adjustments are controllable via a scaling factor, (2) composed image embeddings through semantic transfer from text prompts to image features, and (3) weighted fusion of composed text and image embeddings that enhances retrieval by balancing visual and semantic similarity. Our approach serves as a plug-and-play enhancement for existing ZS-CIR methods with minimal computational overhead. Extensive experiments across multiple benchmarks demonstrate that PDV consistently improves retrieval performance when integrated with state-of-the-art ZS-CIR approaches, particularly for methods that generate accurate compositional embeddings. The code will be publicly available.*

1. Introduction

Composed Image Retrieval (CIR) involves searching for images using a combination of a reference image and a prompt that describes how the target image should differ from the reference [2, 4, 18, 20]. Compared to traditional content-based image retrieval (CBIR) systems, CIR offers increased flexibility and precision by allowing users to articulate complex, multi-modal queries that combine visual and semantic information [6, 11, 18].

The core challenge in CIR lies in effectively integrat-

ing information from two distinct modalities: image and text. With the rapid progress in vision and language models (VLMs), CIR has attracted significant attention in the computer vision community [2, 4, 11, 15, 18]. Early approaches to CIR were primarily supervised in nature [1, 5, 12, 13, 20, 21]. However, as highlighted by Saito et al. [18], the labeling cost for supervised datasets in this domain is prohibitively high, prompting researchers to explore more efficient alternatives, namely zero-shot composed image retrieval (ZS-CIR). In this work, we provide a simple and training-free approach to improve the controllability and accuracy of existing ZS-CIR approaches.

ZS-CIR leverages VLMs, denoted by Ψ , which operate through a dual-pathway architecture. The first pathway consists of a vision branch, Ψ_I , that extracts feature embeddings from target images, I_{target} . The second pathway employs a language branch, Ψ_T , that processes a textual composition of reference images, I_{ref} , and user-provided text prompts, P . This composition, represented by $\mathcal{F}(I_{ref}, P)$, can be achieved through two primary methods: (1) *Caption Generation*, where a caption is generated for the reference image using a VLM, and this caption is merged with the text-prompt using Large Language Models (LLMs), as demonstrated in CIReVL [11]; or (2) *Pseudo Tokenization*, which uses CLIP’s [16] visual branch to process the I_{ref} and a mapping network (consisting of a lightweight multi-layer perceptron) to tokenise the image, as demonstrated in Pic2Word [18]. The resulting $\mathcal{F}(I_{ref}, P)$ is a textual query representation that encompasses both the provided visual and text information, and facilitates zero-shot retrieval. The aforementioned pipeline is illustrated in Figure 1a.

Despite promising results reported in the literature [2, 8, 11, 18], existing approaches include three significant limitations:

Gap 1: Statically Composed Text Embedding. Target images, I_{target} , may not appear in the Top-K retrieved results when other gallery images produce embeddings that are closer to the composed text embedding $\Psi_T(\mathcal{F}(I_{ref}, P))$ than the target image embedding $\Psi_I(I_{target})$, as shown in Figure 1a. In such cases, users must iteratively refine their

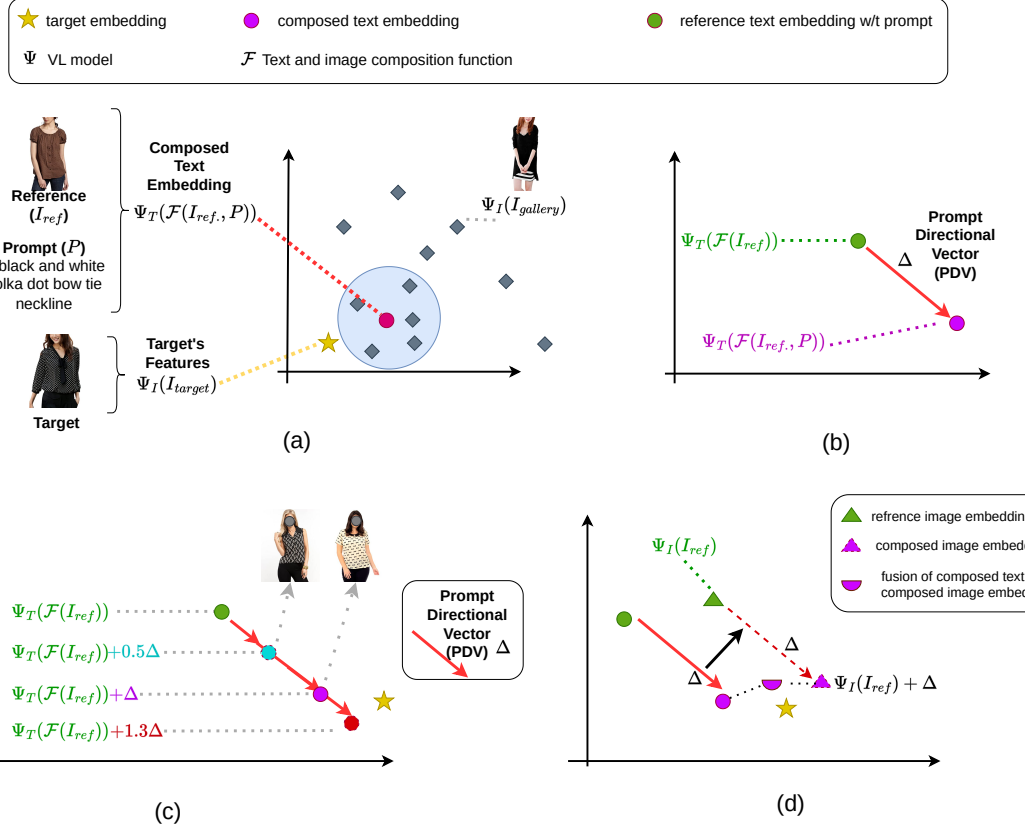


Figure 1. Figure 1: Overview of Prompt Directional Vector (PDV) for Zero-Shot Composed Image Retrieval (ZS-CIR). (a) Standard ZS-CIR pipeline. (b) PDV calculation process. (c) Dynamic text embedding composition using PDV. (d) Fusion of composed embeddings: PDV-modified image embedding combined with composed text embedding.

prompts and regenerate composed text embeddings, incurring additional manual effort and computational overhead.

Gap 2: Underutilisation of Reference Image Embedding. Current methods typically do not leverage the embedding $\Psi_I(I_{ref})$ of the reference image. This omission stems from consistently poor retrieval performance observed when incorporating these embeddings, as documented in multiple studies [2, 11, 18].

Gap 3: Suboptimal Performance of Image-Text Embedding Fusion. While the fusion of image and text embeddings outperforms single-modality approaches (image-only or text-only) [2, 11, 18], it still underperforms compared to composed text embeddings.

Promp Directional Vector (PDV): a Plug-and-Play Solution. We propose a straightforward, training-free approach to address both these challenges by introducing the *Prompt Directional Vector* (PDV). Denoted by Δ_{PDV} , the PDV represents the residual vector between two text embeddings: the composed text embedding $\Psi_T(\mathcal{F}(I_{ref}, P))$ and the reference image text embedding $\Psi_T(\mathcal{F}(I_{ref}))$. The latter is equivalent to $\Psi_T(\mathcal{F}(I_{ref}, P_{Empty}))$, where P_{Empty}

represents an empty input string, corresponding to the unprompted baseline. As illustrated in Figure 1b and shown via a red arrow, this PDV captures the semantic modification induced by the prompt. In the following sections, we demonstrate how the PDV effectively addresses the three aforementioned challenges.

PDV: Addressing Gap 1. To change the static nature of the composed text embedding, we generalise the synthesis of the composed text embeddings $\Psi_T(\mathcal{F}(I_{ref}, P))$. We interpret $\Psi_T(\mathcal{F}(I_{ref}, P))$ as a shift from the reference image text embedding without the prompt, $\Psi_T(\mathcal{F}(I))$, by a vector Δ_{PDV} . Under this formulation, the baseline ZS-CIR approach can be viewed as a special case where $\Psi_T(\mathcal{F}(I_{ref}, P)) = \Psi_T(\mathcal{F}(I_{ref}, P)) + \alpha\Delta_{PDV}$ with $\alpha = 1$. We hypothesize that when Δ_{PDV} captures the desired modifications but not their precise magnitude (particularly with less descriptive prompts), adjusting α can enhance retrieval performance and controllability. As demonstrated in Figure 1c, increasing α to 1.3 produces results more closely aligned with the target compared to the baseline case of $\alpha = 1$.

PDV: Addressing Gap 2. Although image embeddings $\Psi_I(I_{ref})$ contain valuable visual content regarding the reference image, they lack prompt-specific semantic information, leading to poor performance when used in ZS-CIR. By leveraging the shared semantic space learned by Vision-Language models across image and text modalities, we can transfer prompt semantics to the image embedding by adding the Prompt Vector Δ , obtaining $\Psi_I(I_{ref}) + \alpha\Delta_{PDV}$, as illustrated in Figure 1d. We denote this augmented representation as the *composed image embedding*. Similar to the dynamic composed text embedding, this representation can be adjusted through a scaling factor, α .

PDV: Addressing Gap 3. Lastly, several studies demonstrate that the direct fusion of image and text embeddings outperforms using either input feature (image or text-prompt) alone. [2, 11, 18]. However, this fusion approach still underperforms compared to using the composed text embeddings. This performance gap exists because prompt embeddings are significantly changed by incorporating context from the reference image. Specifically, Δ is not equivalent to $\Psi_T(P)$. To address this, we propose fusing the composed text and composed image embeddings, as illustrated in Figure 1d. Through varying the fusion weight factor β , we can control the balance between visual similarity to the reference image and semantic alignment with the prompt. Lower β values prioritize visual fidelity, while higher values emphasize semantic modifications specified in the prompt.

PDV serves as a plug-and-play enhancement for most ZS-CIR approaches, offering a simple and training-free solution. The computational overhead is minimal, requiring only the calculation of text and image embeddings from the reference image. We evaluate PDV by integrating it with two distinct ZS-CIR methods across various CIR benchmarks. Our experimental results demonstrate that all three use cases of PDV consistently improve upon the baseline approaches, particularly when the baseline method already generates accurate compositional embeddings.

Contributions. Our main contributions are as follows:

- We introduce the Prompt Directional Vector (PDV), a simple and training-free enhancement for overcoming the limitations of current Zero-Shot Composed Image Retrieval.
- We propose three novel applications of PDV: (1) dynamic composed text embedding synthesis through PDV scaling, which enhances control over retrieval results, (2) composed image embedding synthesis via semantic transfer from prompts to visual features through PDV addition, which prioritizes visual similarity, and (3) effective fusion of composed text and image embeddings, which improves overall performance and enables controllable balancing of visual and semantic similarity.
- Through extensive experiments on multiple benchmarks with two ZS-CIR methods, we demonstrate that PDV

consistently improves retrieval performance with minimal computational overhead.

2. Related Work

Vision-Language (VL) models have revolutionized computer vision by effectively bridging visual and textual modalities. The emergence of powerful models such as CLIP [16], ALIGN [10], and Florence [23] has enabled remarkable advances in multi-modal understanding. Trained on large-scale image-text pairs through contrastive learning, these models learn rich visual-semantic representations that generalize across domains and tasks. Building upon these advances, Composed Image Retrieval (CIR) has shown significant progress [4, 11, 18]. Early approaches leverage VL models and either trained a combiner network to compose text and image features [4], or fine-tuned a text encoder [3] to extract task-specific text features. However, these methods still require expensive domain-specific triplets (reference image, modified image, and text description) that must be manually verified. Recent work has explored alternative approaches to reduce the data collection burden, such as using synthetic triplets [9] or mining triplets from large-scale image-text datasets [14]. However, these methods still incur significant computational costs during training.

Zero-shot CIR with Text Inversion Recent research has focused on zero-shot approaches to address these challenges. Many methods adopt *text inversion*, a technique initially proposed for personalized image generation [7, 17], which maps images to pseudo tokens or words. Pic2Word [18] introduced a self-supervised text inversion network trained with cyclic contrastive loss, though it requires a large-scale image dataset. SEARLE [2] reduces the cost of training Pic2Word and improves the efficiency of the text inversion network. To further improve scalability, LinCIR [8] proposed a language-only approach that reduces training costs and increases scalability. Most recently, CIReVL [11] introduced a more direct method that leverages image captioning models to generate natural language descriptions of reference images, which are then combined with text that specifies desired modifications to form queries.

Composition with a Residual In contrast to ZS-CIR, early supervised CIR approaches learned prompt-induced modifications by training on labelled triplet data (reference image, prompt, and target image). Vo et al. [20] pioneered this approach by introducing a residual learning module based on an LSTM network. Subsequently, several methods [5, 21, 22] adopted similar residual learning strategies for text-image composition. Baldrati et al. [3] further advanced this approach by fine-tuning CLIP’s text encoder to learn residual embeddings. While these prior works explored residual-based approaches, they all relied on supervised training. In contrast, our proposed PDV achieves similar capabilities by directly leveraging pre-trained VL mod-

els, eliminating the need for task-specific training.

Comparative Summary. While residual embeddings were widely explored in early CIR studies, they were limited to supervised settings. Recent zero-shot approaches have demonstrated that effective CIR systems can be built by leveraging pre-trained VL models without expensive supervised training. However, key challenges persist in controllability, accuracy, and effective multi-modal fusion, which we address in this work.

3. Improved Zero-shot Composed Image Retrieval (ZS-CIR)

3.1. Baseline ZS-CIR Framework

Composed Image Retrieval (CIR) enables users to search for target images I_{target} by providing a reference image, I_{ref} , and a text prompt, P , describing desired modifications. Zero-shot composed image retrieval (ZS-CIR) leverages Vision-Language (VL) models, Ψ , such as CLIP [16], whose vision branch, Ψ_I , and text branch, Ψ_T , are trained to learn a shared embedding space where semantically similar image and text pairs are mapped close to each other. In this framework, target images are encoded using the vision branch, Φ_I , while the query is composed by processing both I_{ref} and P through the text branch Ψ_T , as composition operations are more naturally handled in the text modality.

Recent ZS-CIR approaches generate the composed text embedding from I_{ref} and P using one of two methods: direct image captioning (CIReVL) or pseudo tokenization (Pic2Word). We denote this composition process as \mathcal{F} , resulting in a composed text embedding $\Psi_T(\mathcal{F}(I_{ref}, P))$.

In an ideal ZS-CIR scenario, the target image I_{target} should appear within the top-k results retrieved from the gallery \mathcal{D} . This retrieval is formalized as:

$$\mathbb{I}_{top-k} = \arg \max_{I \in \mathcal{D}} \frac{\Psi_T(\mathcal{F}(I_{ref}, P))^T \cdot \Psi_I(I)}{\|\Psi_T(\mathcal{F}(I_{ref}, P))\| \cdot \|\Psi_I(I)\|}. \quad (1)$$

If $I_{target} \notin \mathbb{I}_{top-k}$, the user must reformulate the prompt and repeat the feature extraction process to obtain alternative retrieval results. Notably, as shown in Eq. 1, only the composed feature embedding $\Psi_T(\mathcal{F}(I_{ref}, P))$ directly influences the computation of \mathbb{I}_{top-k} results. Although the gallery images are represented by their image embeddings, the image embedding of the reference image $\Psi_I(I_{ref})$ does not contribute to the retrieval process.

3.2. Prompt Directional Vector

Rather than simply employing the embedding point alone, $\Psi_T(\mathcal{F}(I_{ref}, P))$, we propose a generalized formulation of composed text embeddings by considering an embedding direction, Δ_{PDV} , which is derived from the difference between the provided prompt, P , and the reference image,

I_{ref} . Formally, we define Δ_{PDV} as,

$$\Delta_{PDV} = \Psi_T(\mathcal{F}(I_{ref}, P)) - \Psi_T(\mathcal{F}(I_{ref})). \quad (2)$$

We then form the composed text embedding as follows,

$$\Psi_T(\mathcal{F}(I_{ref}, P)) = \Psi_T(\mathcal{F}(I_{ref})) + \alpha \Delta_{PDV}, \quad (3)$$

where α controls the movement along the prompt vector Δ_{PDV} and $\Psi_T(\mathcal{F}(I_{ref}))$ is the original text embedding.

3.3. Strategies for Using the Prompt Directional Vector

We explore three strategies to incorporate the Prompt Directional Vector, Δ_{PDV} .

(1) **Prompt Directional Vector for Text (PDV-T)**, which enhances controllability in ZS-CIR. While baseline ZS-CIR approaches represent a special case where $\alpha = 1$, varying α provides users with additional control over the retrieval process. Setting $\alpha > 1$ amplifies the modification specified by the prompt, while $\alpha < 1$ reduces its effect. This approach offers a more efficient alternative to modifying the prompt directly, as it requires neither new feature extraction nor prompt reformulation. Note we use the notation Φ_{PDV-T} to represent the composed text embedding.

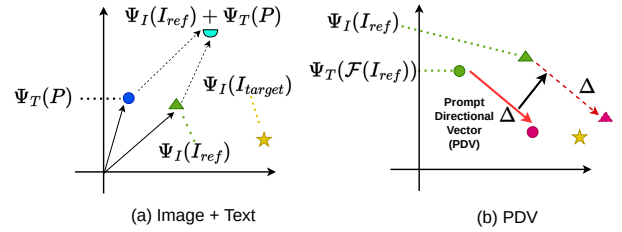


Figure 2. Comparison of Image + Text (a) vs PDV (b).

(2) **Prompt Directional Vector for Image (PDV-I)**, which extends the modification principle to visual embeddings. While previous approaches primarily relied on composed text embeddings, experimental results show that direct fusion of image and text features yields inferior performance compared to composed features. We hypothesize that this performance gap arises because the direct text embedding, $\Phi_T(P)$, differs significantly from the prompt vector Δ_{PDV} , as illustrated in Figure 2. This difference occurs because the semantic meaning of natural language is context-sensitive, where in our case the context is provided by the reference image embedding $\Psi_T(\mathcal{F}(I_{ref}))$. To address this limitation, we propose incorporating Δ_{PDV} into visual embeddings. Specifically, we compute the composed visual embedding Φ_{PV-T} as $\Psi_I(I_{ref}) + \alpha \Delta_{PDV}$, where $\Psi_I(I_{ref})$ represents the original visual embedding of the

reference image, and the same prompt vector obtained via Eq. 2 is used to modify this visual representation.

(3) Prompt Directional Vector Fusion (PDV-F), which calculates the final similarity score between a query and target image which combines both composed embeddings. This fusion embedding, Φ_{PV-F} , can be defined as,

$$\Phi_{PV-F} = (1 - \beta)\Phi_{PV-I} + \beta\Phi_{PV-T}, \quad (4)$$

where β is a weighting parameter balancing the contribution of the composed visual and textual embeddings.

4. Experiments

4.1. Implementation Details

We utilize the official implementations of two baseline methods: CIREVL¹ as a representative caption-based feature extraction approach, and Pic2Word² as a representative pseudo tokenization-based method. All feature extraction processes follow the original implementations provided by these baseline methods. However, to calculate Δ_{PDV} , we need text embeddings without prompts, which are not provided in the original implementations. For CIREVL, we obtain these embeddings by passing the generated image captions directly to CLIP. For Pic2Word, we construct the base text embedding by passing the phrase “a photo of ⟨token⟩” to CLIP, where ⟨token⟩ represents the extracted image token obtained via text inversion.

4.2. Datasets and Base Vision-Language Models

Following previous work, we evaluated our method on a suite of datasets including Fashion-IQ [21], CIRR [15] and CIRCO [2]. Our proposed method is a plug-and-play approach requiring no additional training, leveraging only pre-trained models. For feature extraction, we use three CLIP variants: ViT-B/32, ViT-L/14, and ViT-G/14, and used the same pre-trained weights as used by the baseline methods. For image tokenization, we employ the pre-trained Pic2Word model.

4.3. Effect of Using the PDV

In this section we explore the impact of the three proposed uses of the prompt direction vector (PDV): Using the PDV to augment text queries (PDV-T, see Sec. 4.3.1), using the PDV to augment image queries (PDV-I, see Sec. 4.3.2), and using the PDV in queries that fuse image and text data (PDV-F, see Sec. 4.3.3).

4.3.1 Analysing the PDV for Text (PDV-T)

To investigate how scaling the prompt vector, Δ_{PDV} , affects retrieval performance with composed text embed-

dings, we conducted experiments using two zero-shot approaches (CIREVL and Pic2Word) with different backbone networks across three datasets. We evaluated the performance by varying the scaling parameter, α (Eq. 3), from -0.5 to 3 by an interval of 0.1.

The results are presented in Figure 3a. To account for scale variations across different experiments, we report relative recall values, where a baseline of zero is established at $\alpha = 1$. As shown in Figure 3a, varying α leads to significant changes in relative recall performance³. Our analysis reveals method-specific patterns across datasets. With CIREVL, increasing α improves relative recall on both FashionIQ and CIRCO datasets. In contrast, Pic2Word shows no significant improvement on FashionIQ and CIRR when varying α , while CIRCO’s performance improves when α is reduced to 0.8-1.0. This divergent behavior is fundamentally linked to each method’s ability to generate an accurate Δ_{PDV} . As demonstrated in Tables 2 and 1, CIREVL consistently outperforms Pic2Word across various benchmarks, indicating its superior ability to generate a more accurate composed query, and thus a more accurate Δ_{PDV} . Consequently, increasing α yields greater benefits for CIREVL compared to Pic2Word.

We visualize the top-5 retrieval results using CIREVL with a ViT-B-32 backbone across three datasets (one reference image from each) under varying α values, as shown in Figure 4a. As α increases, the retrieved results show stronger alignment with the prompt. Conversely, when α exceeds 1, the results include semantically related but unseen variations, while α values below 0.5 yields results opposite to the prompt’s intent. For instance, “brighter blue and sleeveless” retrieves “dark blue with sleeves,” “plain background” yields “natural/dark background,” and “young boy” returns “adult” images.

4.3.2 Analysing the PDV for Image (PDV-I)

To evaluate whether Δ_{PDV} enhances the retrieval performance of image embeddings, we conducted experiments following the protocol described in Section 4.3.1. We modified image embeddings by adding Δ_{PDV} scaled with α values ranging from -0.5 to 2.0, where $\alpha = 0$ represents the original image-only embeddings. As shown in Figure 3b, Recall@K exhibits a positive correlation with α for values below 1. This upward trend continues until $\alpha = 2.0$ for CIREVL, while Pic2Word’s performance peaks when α reaches 1.4.

Following the methodology in Section 4.3.1, we conduct similar visualizations, with results shown in Figure 4b. As with PDV-T, increasing α leads to stronger alignment between retrieved results and the prompt. When α exceeds 0.5, the results exhibit semantic relationships to

¹https://github.com/ExplainableML/Vision_by_Language

²https://github.com/google-research/composed_image_retrieval

³See supplementary material for Recall@10 and Recall@50 figures

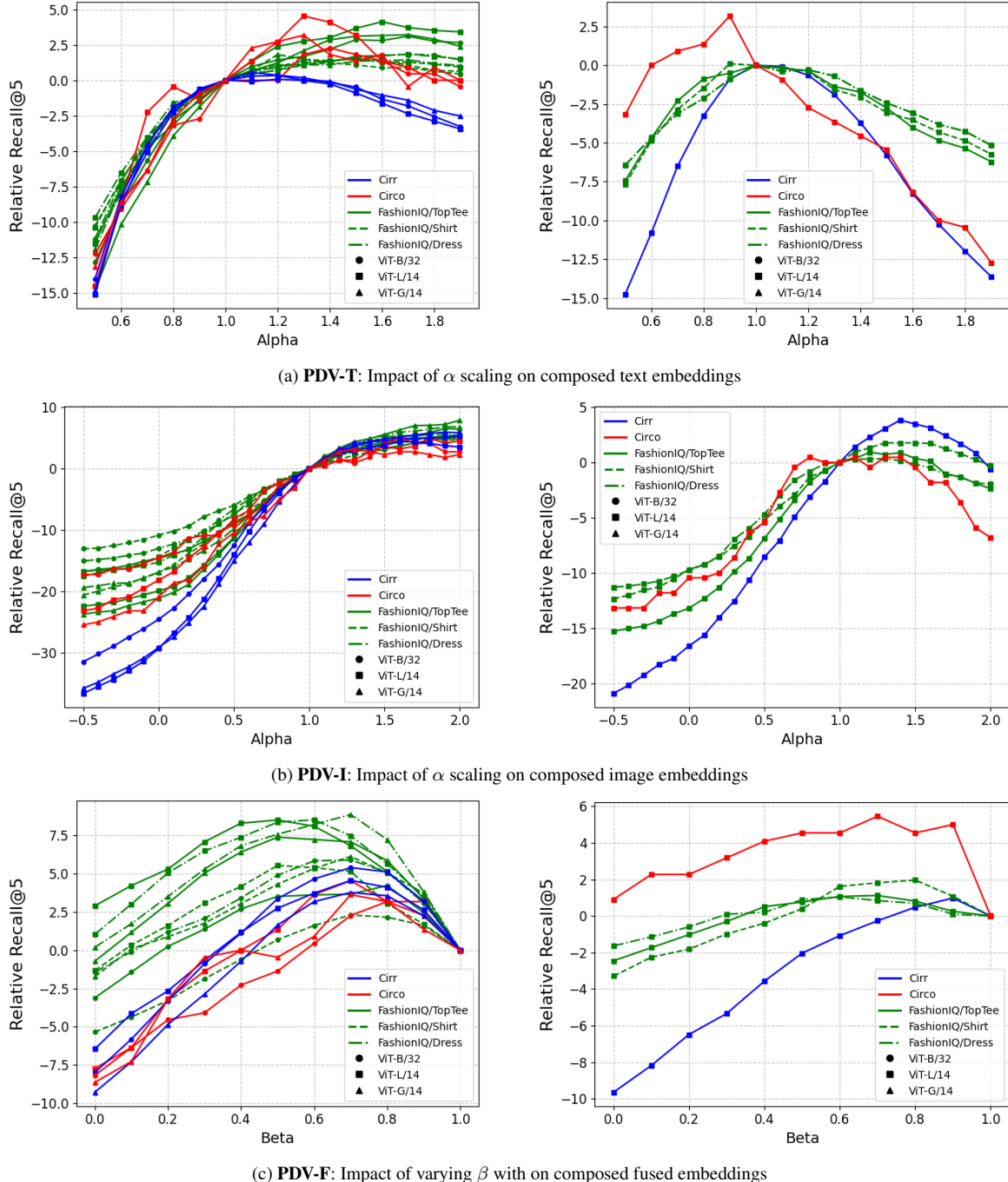


Figure 3. Impact of changing α/β on Recall@5 performance across different PDV applications. For each row, results are shown for the CIReVL (left) and Pic2Word (right) baseline methods.

the query, while α values below 0.5 yield results opposing the prompt’s intent. Notably, PDV-I’s top retrievals demonstrate higher visual similarity to reference images compared to PDV-F, as evidenced by the preserved design elements in the clothing item (left) and laptop (middle). This characteristic is particularly valuable for applications include fashion

search [21] and logo retrieval [19], where visual similarity plays a crucial role.



Figure 4. Visualisation of the impact of α/β scaling to top-5 retrieval results. CIREVL with ViT-B-32 Clip model is the baseline method used. Representative examples with prompts from three datasets: FashionIQ (left), CIRR (middle), and CIRCO (right) are shown at the top. **Green** and **blue** bounding boxes indicate true positives and near-true positives, respectively.

4.3.3 Analysing PDV Fusion (PDV-F)

Finally, we evaluate the effectiveness of fusing image and text-composed embeddings by varying the fusion parameter,

β , from 0 to 1. At $\beta = 0$, the model relies solely on composed image embeddings, while at $\beta = 1$, it uses only composed text embeddings. As shown in Figure 3c,

the fusion of both embeddings consistently outperforms either embedding type alone. Optimal retrieval performance is typically achieved when β is between 0.4 and 0.8.

We similarly visualize the top-5 retrieved results across different β values. As shown in Figure 4c, When β is small, the retrieved results maintain high visual similarity to the reference image. Conversely, as β exceeds 0.5, the results demonstrate stronger semantic alignment with the prompt.

4.4. ZS-CIR Benchmark Comparison

We evaluated PDV-F in combination with two baseline approaches (CIReVL and Pic2Word) across three benchmarks, setting β to 0.7 for CIReVL and 0.9 for Pic2Word based on the fusion ablation results shown in Figure 3c. The results are presented in Tables 1 and 2. On the FashionIQ benchmark, PDV-F yields substantial improvements for both baseline approaches, with CIReVL showing particularly strong gains that scale with backbone size. Similarly, both methods demonstrate significant performance improvements on CIRCO and CIRR datasets. Notably, CIReVL achieves larger improvements compared to Pic2Word, with the most substantial gains observed when using small and medium backbone architectures.

5. Conclusion

We introduce the Prompt Directional Vector (PDV), a simple yet effective approach for enhancing Zero-Shot Composed Image Retrieval. PDV captures semantic modifications induced by user prompts without requiring additional training or expensive data collection. Through extensive experiments across multiple benchmarks, we demonstrated three successful applications of PDV: dynamic text embedding synthesis, composed image embedding through semantic transfer, and effective multi-modal fusion.

Our approach not only improves retrieval performance consistently, but also provides enhanced controllability through the use of scaling factors. PDV serves as a plug-and-play enhancement that can be readily integrated with existing ZS-CIR methods while incurring minimal computational overhead.

We note that PDV’s effectiveness correlates strongly with the underlying method’s ability to generate accurate compositional embeddings. This insight suggests promising future research directions, including developing more robust compositional embedding techniques and exploring adaptive scaling strategies for PDV. The simplicity and effectiveness of PDV also open possibilities for its application in multi-prompt composed image retrieval (*i.e.* dialogue-based search) and other multi-modal tasks where semantic modifications play a crucial role.

A. Appendix

In this section, we present additional quantitative results.

A.0.1 Ablation Analysis

While Figure 3 in the main paper illustrates the effects of scaling factor α and fusion factor β on Recall@5 performance across various PDV applications, Figures 5, 6, and 7 present complementary results for Recall@10 and Recall@50 metrics.

The Recall@10 and Recall@50 results demonstrate consistent trends with the Recall@5 findings presented in the main paper, thus validating our conclusions across multiple evaluation metrics.

A.0.2 ZS-CIR Benchmark Comparison

We also provide additional results achieved on the test set of CIRCO and CIRR datasets (see Table 3), and the validation set of FashionIQ (see Table 4).

- We evaluate PDV integrated with SEARLE [2], a variant of Pic2Word, but more focussed on the salient object in the given image. In this implementation, PDV-F’s β parameter is set to 0.8 across all three datasets, though ablation studies (Figure 7) suggest this value may not be optimal for all scenarios.
- We provide detailed performance breakdowns for individual sub-datasets within FashionIQ in Table 4.
- The optimal performance achieved by both PDV-I and PDV-F on the FashionIQ validation datasets is presented in Table 4.

PDV-T and PDV-F enhance the performance of all three baseline approaches on the FashionIQ dataset. While PDV-I does not improve upon text-inversion methods like Pic2Word and SEARLE, its results significantly outperform image-only baselines and contribute to fusion results that exceed baseline performance.

In contrast, PDV-F demonstrates improved performance over CIReVL and Pic2Word on both CIRCO and CIRR datasets, though it fails to enhance SEARLE’s results. We hypothesize this limitation stems from SEARLE’s single object oriented text inversion approach, which may be less effective for the CIRCO and CIRR datasets which contain multiple objects and complex scenes. This characteristic explains why PDV-F successfully improves the performance of SEARLE in FashionIQ, which features simpler compositions, but not in the CIRCO and CIRR datasets.

Dataset		CIRCO				CIRR						
Arch	Metric Method	mAP@k				Recall@k				R_s @k		
		k=5	k=10	k=25	k=50	k=1	k=5	k=10	k=50	k=1	k=2	k=3
ViT-B/32	Image-only †	1.34	1.60	2.12	2.41	6.89	22.99	33.68	59.23	21.04	41.04	60.31
	Text-only †	2.56	2.67	2.98	3.18	21.81	45.22	57.42	81.01	62.24	81.13	90.70
	Image + Text †	2.65	3.25	4.14	4.54	11.71	35.06	48.94	77.49	32.77	56.89	74.96
	PALAVRA †	4.61	5.32	6.33	6.80	16.62	43.49	58.51	83.95	41.61	65.30	80.94
	SEARLE †	9.35	9.94	11.13	11.84	24.00	53.42	66.82	89.78	54.89	76.60	88.19
	CIReVL †	14.94	15.42	17.00	17.82	23.94	52.51	66.0	86.95	60.17	80.05	90.19
	CIReVL + PDV-F	15.26	16.19	18.16	19.10	31.93	64.19	75.16	92.58	61.86	81.11	90.84
ViT-L/14	Pic2Word	6.81	7.49	8.51	9.07	23.69	51.32	63.66	86.21	53.61	74.34	87.28
	Pic2Word + PDV-F	7.77	8.70	9.80	10.42	23.81	51.86	64.34	86.84	52.58	73.54	86.89
	SEARLE †	11.68	12.73	14.33	15.12	24.24	52.48	66.29	88.84	53.76	75.01	88.19
	CIReVL †	18.57	19.01	20.89	21.80	24.55	52.31	64.92	86.34	59.54	79.88	89.69
ViT-G/14	CIReVL †	26.77	27.59	29.96	31.03	34.65	64.29	75.06	91.66	67.95	84.87	93.21
	CIReVL + PDV-F	25.24	26.80	29.47	30.56	36.75	67.54	76.99	93.18	65.06	82.53	91.74

Table 1. Performance comparison on CIRCO and CIRR test datasets across different backbone architectures. For CIRCO, mAP@k is reported, while for CIRR both Recall@k and Rs@k metrics are used. †denotes that numbers are taken from the original paper.

Backbone	Method	R@10	R@50
ViT-B/32	Image-only †	5.90	13.37
	Text-only †	18.70	36.84
	Image + Text	14.78	29.60
	PALAVRA †	19.76	37.25
	SEARLE †	22.89	42.53
	CIReVL †	28.29	49.35
	CIReVL + PDV-F	33.82	54.94
ViT-L/14	Pic2Word †	24.70	43.70
	Pic2Word + PDV-F	26.12	45.26
	SEARLE †	25.56	46.23
	CIReVL †	28.55	48.57
ViT-G/14	CIReVL + PDV-F	36.78	56.82
	CIReVL †	32.19	52.36
	CIReVL + PDV-F	41.72	61.39

Table 2. Comparison of average recall values of different methods on Fashion-IQ validation dataset using various backbone models. †denotes that numbers are taken from the original paper.

References

- [1] Muhammad Umer Anwaar, Egor Labintcev, and Martin Kleinstueber. Compositional learning of image-text query for image retrieval. In *Proceedings of the IEEE/CVF Winter conference on Applications of Computer Vision*, pages 1140–1149, 2021. 1
- [2] Alberto Baldrati, Lorenzo Agnolucci, Marco Bertini, and Alberto Del Bimbo. Zero-shot composed image retrieval with textual inversion. In *Proceedings of the IEEE/CVF International Conference on Computer Vision*, pages 15338–15347, 2023. 1, 2, 3, 5, 8
- [3] Alberto Baldrati, Marco Bertini, Tiberio Uricchio, and Alberto Del Bimbo. Conditioned and composed image retrieval combining and partially fine-tuning clip-based features. In *Proceedings of the IEEE/CVF Conference on Computer Vision and Pattern Recognition*, pages 4959–4968, 2022. 3
- [4] Alberto Baldrati, Marco Bertini, Tiberio Uricchio, and Alberto Del Bimbo. Effective conditioned and composed image retrieval combining clip-based features. In *Proceedings of the IEEE/CVF conference on computer vision and pattern recognition*, pages 21466–21474, 2022. 1, 3
- [5] Yanbei Chen and Loris Bazzani. Learning joint visual semantic matching embeddings for language-guided retrieval. In *Computer Vision–ECCV 2020: 16th European Conference, Glasgow, UK, August 23–28, 2020, Proceedings, Part XXII 16*, pages 136–152. Springer, 2020. 1, 3
- [6] Niv Cohen, Rinon Gal, Eli A Meirom, Gal Chechik, and Yuval Atzmon. “this is my unicorn, fluffy”: Personalizing frozen vision-language representations. In *European conference on computer vision*, pages 558–577. Springer, 2022. 1
- [7] Rinon Gal, Yuval Alaluf, Yuval Atzmon, Or Patashnik, Amit H. Bermano, Gal Chechik, and Daniel Cohen-Or. An image is worth one word: Personalizing text-to-image generation using textual inversion, 2022. 3
- [8] Geonmo Gu, Sanghyuk Chun, Wonjae Kim, , Yoohoon Kang, and Sangdoo Yun. Language-only training of zero-shot composed image retrieval. In *Conference on Computer Vision and Pattern Recognition (CVPR)*, 2024. 1, 3
- [9] Geonmo Gu, Sanghyuk Chun, Wonjae Kim, HeeJae Jun, Yoohoon Kang, and Sangdoo Yun. Compodiff: Versatile composed image retrieval with latent diffusion. *arXiv preprint arXiv:2303.11916*, 2023. 3
- [10] Chao Jia, Yinfai Yang, Ye Xia, Yi-Ting Chen, Zarana Parekh, Hieu Pham, Quoc Le, Yun-Hsuan Sung, Zhen Li, and Tom Duerig. Scaling up visual and vision-language representation learning with noisy text supervision. In *International conference on machine learning*, pages 4904–4916. PMLR, 2021. 3
- [11] Shyamgopal Karthik, Karsten Roth, Massimiliano Mancini, and Zeynep Akata. Vision-by-language for training-free compositional image retrieval. *International Conference on Learning Representations (ICLR)*, 2024. 1, 2, 3

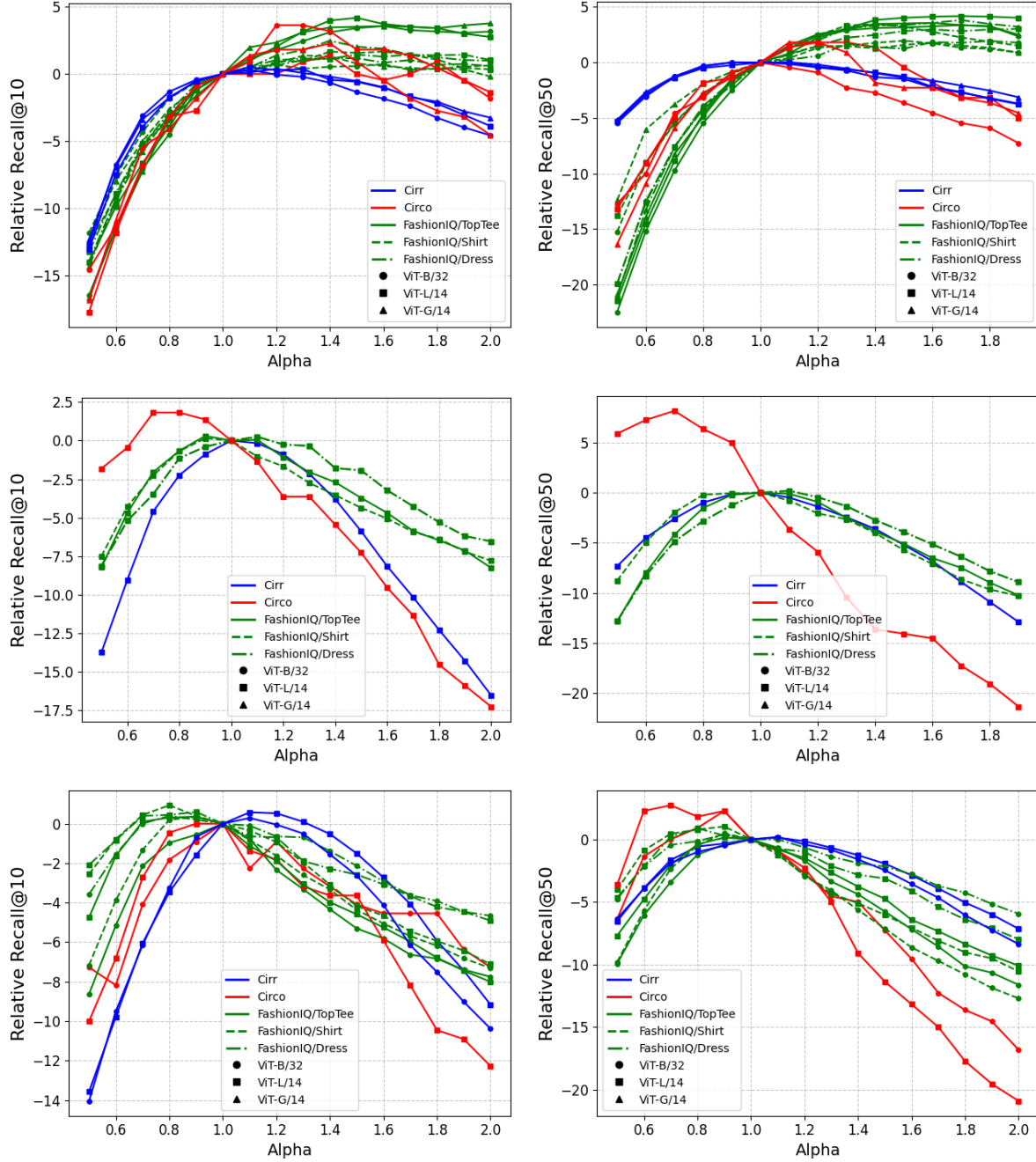


Figure 5. PDV-T: Impact of α scaling on Recall@10 (left) and Recall@50 (right) performance. Results shown for three baseline methods: CIReVL (top), Pic2Word (middle) and SEARLE (bottom).

- [12] Jongseok Kim, Youngjae Yu, Hoeseong Kim, and Gunhee Kim. Dual compositional learning in interactive image retrieval. In *Proceedings of the AAAI Conference on Artificial Intelligence*, volume 35, pages 1771–1779, 2021. 1
- [13] Seungmin Lee, Dongwan Kim, and Bohyung Han. Cosmo: Content-style modulation for image retrieval with text feedback. In *Proceedings of the IEEE/CVF Conference on Computer Vision and Pattern Recognition*, pages 802–812, 2021.

- [14] Yikun Liu, Jiangchao Yao, Ya Zhang, Yanfeng Wang, and Weidi Xie. Zero-shot composed text-image retrieval. *arXiv preprint arXiv:2306.07272*, 2023. 3
- [15] Zheyuan Liu, Cristian Rodriguez-Opazo, Damien Teney, and Stephen Gould. Image retrieval on real-life images with pre-

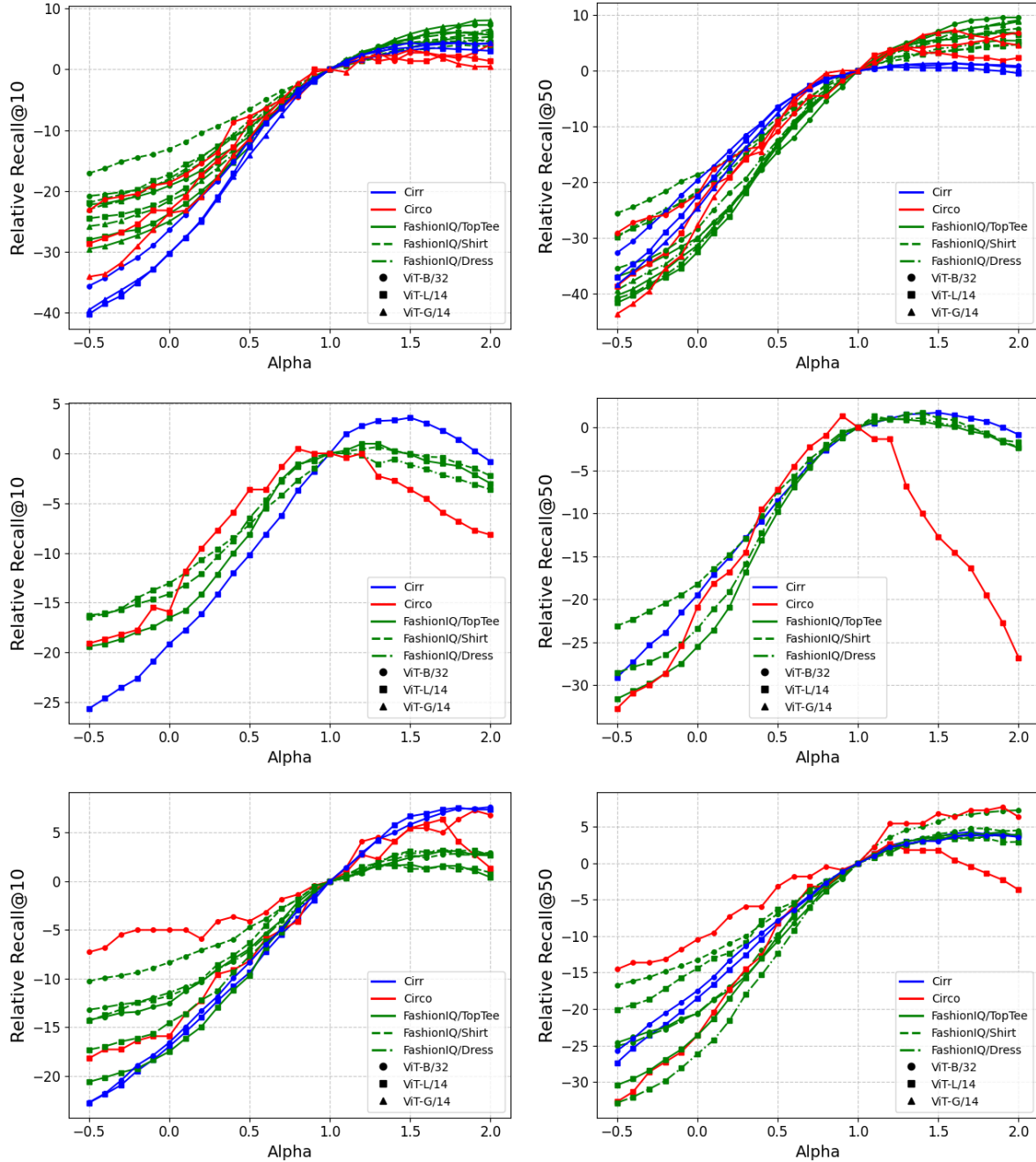


Figure 6. PDV-I: Impact of α scaling on Recall@10 (left) and Recall@50 (right) performance. Results shown for three baseline methods: CIREVL (top), PIC2WORD (middle) and SEARLE (bottom).

- trained vision-and-language models. In *Proceedings of the IEEE/CVF International Conference on Computer Vision*, pages 2125–2134, 2021. 1, 5
- [16] Alec Radford, Jong Wook Kim, Chris Hallacy, Aditya Ramesh, Gabriel Goh, Sandhini Agarwal, Girish Sastry, Amanda Askell, Pamela Mishkin, Jack Clark, et al. Learning transferable visual models from natural language supervi-

- sion. In *International conference on machine learning*, pages 8748–8763. PMLR, 2021. 1, 3, 4
- [17] Nataniel Ruiz, Yuanzhen Li, Varun Jampani, Yael Pritch, Michael Rubinstein, and Kfir Aberman. Dreambooth: Fine tuning text-to-image diffusion models for subject-driven generation. In *Proceedings of the IEEE/CVF conference on computer vision and pattern recognition*, pages 22500–

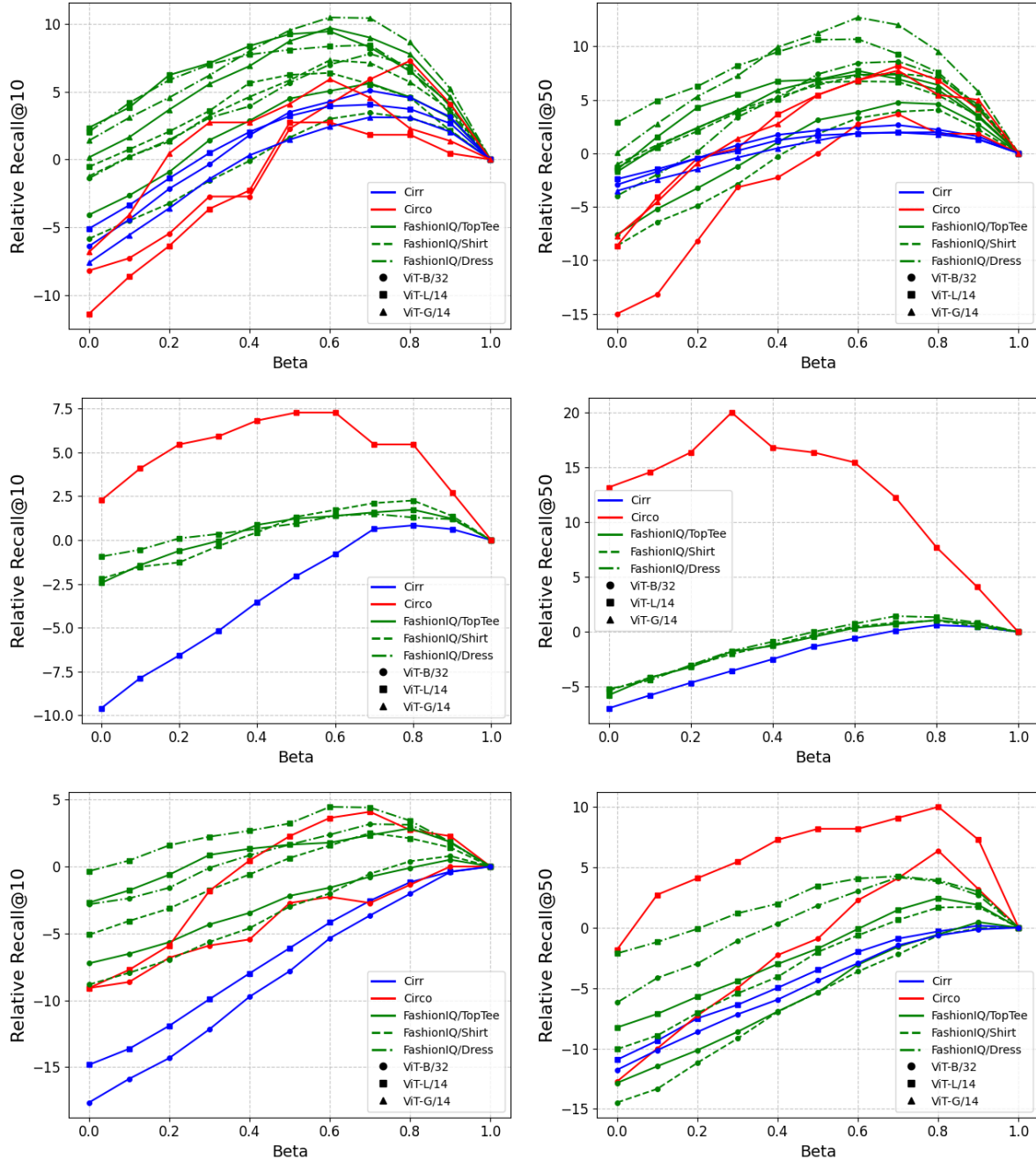


Figure 7. PDV-F: Impact of β scaling on Recall@10 (left) and Recall@50 (right) performance. Results shown for three baseline methods: CIReVL (top), Pic2Word (middle) and SEARLE (bottom).

- 22510, 2023. 3
- [18] Kuniaki Saito, Kihyuk Sohn, Xiang Zhang, Chun-Liang Li, Chen-Yu Lee, Kate Saenko, and Tomas Pfister. Pic2word: Mapping pictures to words for zero-shot composed image retrieval. In *Proceedings of the IEEE/CVF Conference on Computer Vision and Pattern Recognition*, pages 19305–19314, 2023. 1, 2, 3

- [19] Osman Tursun, Simon Denman, Sabesan Sivapalan, Sridha Sridharan, Clinton Fookes, and Sandra Mau. Component-based attention for large-scale trademark retrieval. *IEEE Transactions on Information Forensics and Security*, 17:2350–2363, 2019. 6
- [20] Nam Vo, Lu Jiang, Chen Sun, Kevin Murphy, Li-Jia Li, Li Fei-Fei, and James Hays. Composing text and image

Dataset		CIRCO				CIRR						
Arch	Metric Method	mAP@k				Recall@k				R_s @k		
		k=5	k=10	k=25	k=50	k=1	k=5	k=10	k=50	k=1	k=2	k=3
ViT-B/32	Image-only †	1.34	1.60	2.12	2.41	6.89	22.99	33.68	59.23	21.04	41.04	60.31
	Text-only †	2.56	2.67	2.98	3.18	21.81	45.22	57.42	81.01	62.24	81.13	90.70
	Image + Text †	2.65	3.25	4.14	4.54	11.71	35.06	48.94	77.49	32.77	56.89	74.96
	PALAVRA †	4.61	5.32	6.33	6.80	16.62	43.49	58.51	83.95	41.61	65.30	80.94
	SEARLE †	9.35	9.94	11.13	11.84	24.00	53.42	66.82	89.78	54.89	76.60	88.19
	SEARLE + PDV-F	7.26	8.12	9.4	10.12	22.0	51.40	65.18	88.92	50.17	72.75	88.92
	CIReVL †	14.94	15.42	17.00	17.82	23.94	52.51	66.0	86.95	60.17	80.05	90.19
ViT-L/14	CIReVL + PDV-F	15.26	16.19	18.16	19.10	31.93	64.19	75.16	92.58	61.86	81.11	90.84
	Pic2Word	6.81	7.49	8.51	9.07	23.69	51.32	63.66	86.21	53.61	74.34	87.28
	Pic2Word + PDV-F	7.77	8.70	9.80	10.42	23.81	51.86	64.34	86.84	52.58	73.54	86.89
	SEARLE †	11.68	12.73	14.33	15.12	24.24	52.48	66.29	88.84	53.76	75.01	88.19
	SEARLE + PDV-F	10.25	11.53	13.5	14.32	23.08	51.33	64.70	88.34	50.27	72.70	86.05
ViT-G/14	CIReVL †	18.57	19.01	20.89	21.80	24.55	52.31	64.92	86.34	59.54	79.88	89.69
	CIReVL + PDV-F	21.19	22.49	24.67	25.74	34.92	66.58	76.27	92.94	63.95	83.11	92.02
ViT-G/14	CIReVL †	26.77	27.59	29.96	31.03	34.65	64.29	75.06	91.66	67.95	84.87	93.21
	CIReVL + PDV-F	25.24	26.80	29.47	30.56	36.75	67.54	76.99	93.18	65.06	82.53	91.74

Table 3. Performance comparison on the CIRCO and CIRR test datasets across different backbone architectures. For CIRCO, mAP@k is reported, while for CIRR both Recall@k and R_s @k metrics are used. †denotes that numbers are taken from the original paper.

- for image retrieval—an empirical odyssey. In *Proceedings of the IEEE/CVF conference on computer vision and pattern recognition*, pages 6439–6448, 2019. 1, 3
- [21] Hui Wu, Yupeng Gao, Xiaoxiao Guo, Ziad Al-Halah, Steven Rennie, Kristen Grauman, and Rogerio Feris. Fashion iq: A new dataset towards retrieving images by natural language feedback. In *Proceedings of the IEEE/CVF Conference on computer vision and pattern recognition*, pages 11307–11317, 2021. 1, 3, 5, 6
- [22] Youngjae Yu, Seunghwan Lee, Yuncheol Choi, and Gunhee Kim. Curlingnet: Compositional learning between images and text for fashion iq data. *arXiv preprint arXiv:2003.12299*, 2020. 3
- [23] Lu Yuan, Dongdong Chen, Yi-Ling Chen, Noel Codella, Xiyang Dai, Jianfeng Gao, Houdong Hu, Xuedong Huang, Boxin Li, Chunyuan Li, et al. Florence: A new foundation model for computer vision. *arXiv preprint arXiv:2111.11432*, 2021. 3

Fashion-IQ			Shirt		Dress		Toptee		Average	
Backbone	Method	R@10	R@50	R@10	R@50	R@10	R@50	R@10	R@50	
ViT-B/32	Image-only †	6.92	14.23	4.46	12.19	6.32	13.77	5.90	13.37	
	Text-only †	19.87	34.99	15.42	35.05	20.81	40.49	18.70	36.84	
	Image + Text †	13.44	26.25	13.83	30.88	17.08	31.67	14.78	29.60	
	PALAVRA †	21.49	37.05	17.25	35.94	20.55	38.76	19.76	37.25	
	SEARLE	24.14	41.81	18.39	38.08	25.91	47.02	22.81	42.30	
	SEARLE + PDV-T	24.48	42.30	18.79	38.47	25.91	47.02	23.03	42.60	
	SEARLE + PDV-I	18.25	32.14	18.74	39.17	21.77	38.45	19.59	36.59	
	SEARLE + PDV-F	24.53	41.17	21.52	41.89	25.80	46.46	23.95	43.17	
	CIReVL †	28.36	47.84	25.29	46.36	31.21	53.85	28.29	49.35	
	CIReVL + PV-T	29.34	48.92	26.23	48.24	34.57	57.52	30.04	51.56	
ViT-L/14	CIReVL + PV-I	28.95	45.88	29.00	49.13	34.22	56.09	30.72	50.37	
	CIReVL + PV-F	32.04	51.03	32.82	54.88	36.61	58.90	33.82	54.94	
	Pic2Word	25.96	43.52	19.63	40.90	27.28	47.83	24.29	44.08	
	Pic2Word + PV-T	26.10	43.52	19.88	41.10	27.59	47.83	24.52	44.15	
	Pic2Word + PV-I	24.39	39.89	18.69	36.79	25.80	43.04	22.96	39.91	
	Pic2Word + PV-F	28.21	44.55	21.12	42.34	29.02	48.90	26.12	45.26	
	SEARLE	26.84	45.19	20.08	42.19	28.40	49.62	25.11	45.67	
	SEARLE + PDV-T	27.77	46.22	20.67	43.08	28.67	49.77	25.70	46.36	
	SEARLE + PDV-I	23.50	38.71	22.95	44.03	27.43	45.49	24.63	42.74	
	SEARLE + PDV-F	28.95	46.86	23.50	46.11	31.26	52.07	27.90	48.35	
ViT-G/14*	CIReVL †	29.49	47.40	24.79	44.76	31.36	53.65	28.55	48.57	
	CIReVL + PV-T	32.14	50.39	26.33	47.84	34.93	57.88	31.13	52.04	
	CIReVL + PV-I	33.95	50.39	31.73	53.00	39.16	59.95	34.95	54.45	
	CIReVL + PV-F	36.85	53.68	33.32	55.38	40.18	61.40	36.78	56.82	
	CIReVL †	33.71	51.42	27.07	49.53	35.80	56.14	32.19	52.36	
	CIReVL + PV-T	35.57	52.45	30.34	53.00	39.42	60.43	35.11	55.29	
	CIReVL + PV-I	37.78	54.32	35.85	58.25	43.86	63.95	39.16	58.84	
	CIReVL + PV-F	41.51	58.10	38.32	61.87	45.33	64.20	41.72	61.39	

Table 4. Comparison of average recall values of different methods on Fashion-IQ validation dataset using various backbone models. †denotes that numbers are taken from the original paper..